

# HYBRID MAXIMUM CONTROL STRUCTURE USING FUZZY LOGIC OF ELECTRIC VEHICLE

O. KRAA<sup>1</sup>, A. ABOUBOU<sup>1</sup>, M.Y. AYAD<sup>2</sup>, R.SAADI<sup>1</sup>, H. GHODBANE<sup>1</sup>

<sup>1</sup> Laboratory of Energy Systems Modeling, Mohamed Kheider University

<sup>2</sup> Industrial Hybrid Vehicle Applications France

[o.kraa@mselab.org](mailto:o.kraa@mselab.org)

## ABSTRACT

This paper presents a Modelling of traction control system of an Electric Vehicle (EV) based on the Energetic Macroscopic Representation (EMR) and the Maximum Control Structure (MCS). This last is using Fuzzy Logic Control (FLC) to invert the EMR accumulation element for the control task. A developed combination of fuzzy control strategy with SMC combines the advantages of these two approaches and facilitates the inversion of the accumulation elements. In order to validate the simulation results, a comparison between the results obtained by MCS using IP controller which has already been developed by L2EP laboratory (Lille, France) and the presented MSC-FLC obtained by Matlab/Simulink software tool is included.

**INDEX TERMS:** Energetic Macroscopic Representation, Maximum Control Structure, Fuzzy Logic Control, Electric Vehicle, Control Traction.

## 1 INTRODUCTION

Recently the development of the new generation vehicle which is more efficient and less air polluting is accomplished actively. This vehicle generation development can be divided in two axes, one is the Electric Vehicle (EV) and the other is the Hybrid Electric Vehicle (HEV). EVs may be particularly well suited to fleet applications and commuter/town cars. To use EVs in fleets as a practical solution, it is necessary to have technical feasibility and commercial viability that meets the user's needs and affordability. The EV must first be safe, reliable and cost effective, with consistency of the battery system being the key to determine the usefulness as a fleet vehicle [1,2]. In order to answer to the new constraints of study of more complex electromechanical systems, an Energetic Macroscopic Representation (EMR) was proposed. The EMR has been first developed by L2EP laboratory (Lille, France) [19] and has been applied to energetic and multi-physic systems by Femto-ST CNRS Lab (Belfort, France). It does not have the role to replace the traditional representations, but rather to supplement them by a more overall view. The Maximum Control Structure (MCS) results directly from an inversion of the considered EMR modelling. In this paper, a methodology of Fuzzy Logic Control (FLC) is adopted to invert the accumulation element in MCS. Fuzzy logic systems (FLSs) have been credited in control system and applications as powerful

tools capable of providing robust controllers for mathematically ill-defined systems that may be subjected to structured and unstructured uncertainties.

This paper is started by a description of EV structure. In section III, the EMR of the studied system is detailed. Indeed, the proposed MCS and FLC are deduced in section IV and V successively. The Final section of this work presents some results obtained with the proposed control traction. The simulation results of different MCSs are compared in order to exhibit the advantages and disadvantages of each one of them.

## 2 ELECTRIC VEHICLE STRUCTURE

There are several types of motorization for electric traction. At present time, the Direct Current Machines (DCM), and more particularly, separated excitation or permanent magnet synchronous motor are the most widely used. Because of its ease of operation and low cost. The studied vehicle is driven by one DCM with a differential mechanical device. The DCM is supplied by a battery through a DC/DC converter. The Fig. 2 illustrates the EV structure which couples the dynamics of vehicle to electrical motorization.

### 3 ENERGETIC MACROSCOPIC REPRESENTATION OF EV

The EMR has several advantages: it allows the representation of multi-physic systems and the control structures is obtained as a systematic process deduction by inverting simply the EMR bloc by bloc from the controlled output back to the control signal [12]. The EMR formalism has already been used in many real-world applications such as for fuel cell control systems [3], control of hybrid vehicle [8] and control of wind energy generation systems [4]. The studied vehicle is composed of two parts (Fig 2). The first one is the electrical part, it includes a DC voltage source (battery), a DC/DC chopper and a DCM. The second one is the mechanical part, this part includes a differential (coupling components) device, a chassis and a mechanical source. The studied EV EMR is coming from [10].

#### 3.1 Modelling of the components of electric part

##### 3.1.1 Battery

The battery can be modelled as an equivalent circuit such as a voltage source in serial with an internal resistor. The following equation allows to find numerical value of the SOC.

$$SOC(t) = SOC(0) - \frac{100}{C_N} \int I_{bat}(t) dt \quad (1)$$

Where  $SOC(0)$  is initial battery SOC,  $C_N$  is the Nominal battery Capacitance and  $I_{bat}$  is the battery current.

##### 3.1.2 Chopper

Chopper is an electric converter (without energy accumulation and supposed without losses). It is represented as a conversion element (square pictogram), the relationships of the chopper are:

$$\begin{cases} U_{chop} = \alpha_{chop} V_{bat} \\ I_{chop} = \frac{1}{\alpha_{chop}} I_{bat} \end{cases} \quad (2)$$

Where  $\alpha_{chop}$  is chopper amplification gain where  $\alpha_{chop} = \frac{1}{1-\alpha}$  and  $\alpha$  is the duty ratio.  $I_{chop}$ ,  $U_{chop}$  are the chopper current and voltage and  $V_{bat}$  is the battery voltage.

##### 3.1.3 Direct Current Machine

DCM is modelled with classical relationships. The armature current ( $I_{arm}$ ) is the state variable of armature windings and is obtained from the supply voltage and the electromotive force ( $e_{em}$ ):

$$L_{arm} \frac{dI_{arm}}{dt} = U_{chop} - e_{em} - R_{arm} I_{arm} \quad (3)$$

Where  $R_{arm}$  and  $L_{arm}$  are the resistance and inductance of the armature windings. This device is thus an accumulation element due to the presence of the inductance (integration). An electromechanical conversion links both currents to the produce motor torque  $T_{mot}$ . As shown in (4) the  $e_{em}$  is also deduced from the nominal rotation speed  $\Omega_{nom}$ [5-7]:

$$\begin{cases} T_{mot} = k\Phi I_{aarm} \\ e_{em} = k\Phi \Omega_{nom} \\ k\Phi = \frac{U_{arm}^{nom} - R_{arm} I_{arm}^{nom}}{\Omega_{nom}} \end{cases} \quad (4)$$

Where  $k$  is the machine constant parameter related to the torque and to the e.m.f.  $\Phi$  is the magnetic flux. The following equation allows to find the numerical value for the mechanical conversion (shaft + gearbox).

$$\begin{cases} T_{gear} = k_{gear} T_{mot} \\ \Omega_{mot} = k_{gear} \Omega_{gear} \end{cases} \quad (5)$$

Where  $T_{gear}$  and  $\Omega_{gear}$  are the torque and speed rotation after reduction,  $k_{gear}$  is the gearbox reduction coefficient and  $\Omega_{mot}$  is motor rotation speed.

#### 3.2 Modelling of the components of mechanical part

##### 3.2.1 Differential mechanical

The torque reduction is shared fairly on the left and the right wheel, just as the speed of rotation as shown in (6).

$$\begin{cases} T_{diff_{left}} = \frac{1}{2} T_{gear} \\ T_{diff_{right}} = \frac{1}{2} T_{gear} \\ \Omega_{diff} = \frac{1}{2} (\Omega_{left} + \Omega_{right}) \end{cases} \quad (6)$$

Where  $\Omega_{diff}$ ,  $T_{diff_{left}}$  and  $T_{diff_{right}}$  are the differential speed rotation, left and right torque after differential.

##### 3.2.2 Left and right wheels

The wheels have to produce a linear motion from a rotational motion. The traction forces can be calculated from the torque of differential, and the wheel rotation from the vehicle velocity [6, 7, 14].

$$\left\{ \begin{array}{l} F_{left} = \frac{1}{R_{weel}} T_{diff_{left}} \\ w_{left} = \frac{1}{R_{weel}} v_{veh_{left}} \\ F_{right} = \frac{1}{R_{weel}} T_{diff_{right}} \\ w_{right} = \frac{1}{R_{weel}} v_{veh_{right}} \end{array} \right. \quad (7)$$

where  $R_{weel}$  is the radius of wheel,  $F_{left}$ ,  $w_{left}$ ,  $F_{right}$  and  $w_{right}$  are the forces and speed rotations for the left and right wheels, respectively.

### 3.2.3 Mechanical coupling

Both traction forces  $F_{lef}$  and  $F_{right}$  are coupled to produce the total traction force  $F_{tot}$  as shown in (8). By differentiating linear velocities of both the left and right wheels, one can take into account the radius of curvature ( $R_{courb}$ ) and the width of the vehicle ( $l_{veh}$ ) (distance between the rear wheels) [11]

$$\left\{ \begin{array}{l} F_{tot} = k_{left} + F_{right} \\ v_{veh_{left}} = \frac{R_{courb} + \frac{l_{veh}}{2}}{R_{courb}} v_{veh} \\ v_{veh_{right}} = \frac{R_{courb} - \frac{l_{veh}}{2}}{R_{courb}} v_{veh} \end{array} \right. \quad (8)$$

### 3.2.4 Chassis

The vehicle velocity  $V_{veh}$  is obtained with the classical dynamics relationship from the traction force  $F_{tot}$  and  $F_{res}$  as shown in (9):

$$M \frac{dv_{veh}}{dt} = F_{tot} - F_{res} \quad (9)$$

where  $M$  is the mass of vehicle. The chassis is an accumulation element, hence the velocity is chosen as a state variable.

### 3.2.5 Environment

The external environment of the vehicle is considered as a mechanical load and is modelled in EMR with a mechanical source element which is used for both source and load. It yields a resistive force  $F_{res}$  to the motion from the vehicle velocity.

$$F_{res} = \frac{1}{2} \rho \zeta_x S_{front} v_{veh}^2 \quad (10)$$

where  $\rho$ ,  $\zeta_x$  and  $S_{front}$  are the density of air, the vehicle penetration coefficient and the vehicle front surface.

## 4 MAXIMUM CONTROL STRUCTURE OF THE STUDIED VEHICLE

The MCS is composed of several inversion blocks and different REM parts. Then, the EMR blocks are inverted regardless of practical issues: the conversion blocks are directly inverted and the accumulation blocks are inverted using controllers in order to respect physical causality [7,10,11]. In this work, an FLC strategy will be adopted to invert the accumulation element in MCS.

### 4.1 Inversion of standard elements

Mechanical differential and reduction elements are directly inverted to obtain the reference of the duty ratio.

### 4.2 Inversion of chassis

The inversion of the accumulation element associated with the chassis (9) leads to a velocity controller [7-10]:

$$F_{tot_{Ref}} = Con(V_{veh_{Ref}} - V_{veh_{mes}}) \quad (11)$$

where  $Con(x_{ref} - x_{mes})$  is the controller of the variable  $x$ . In this paper, two different control methods are presented. The first one is proposed by [11] and is using the IP (Integral + Proportional). The second one is proposed by authors, it is the FLC which is developed in section 5. [7]

### 4.3 Inversion of Armature

The inversion of the armature winding (3) leads to the armature current controller IP and the e.m.f.  $e_{em}$  compensation [10].

$$U_{chop_{Ref}} = Con(I_{arm_{Ref}} - I_{arm_{mes}}) + e_{em} \quad (12)$$

### 4.4 Inversion of chopper

The chopper has a time-invariant relationship. Consequently, its mathematical relationship is directly inverted to obtain the reference of the duty ratio  $\alpha_{chpRef}$ :

$$\alpha_{chop} = \frac{U_{chop_{Ref}}}{V_{bat_{mes}}} \quad (13)$$

The classical inversion of accumulation bloc using the PI or IP controller needs the calculation of the controller parameters (integral and proportional gains). This task is not obvious and parameters are constant whatever the

vehicle mode is (economic or dynamic). In order to overcome this problem, authors propose to use the FL technique instead of the PI or IP controller which provides an easy and parametric way to control the system and to adjust the vehicle mode.

## 5 DEVELOPMENT OF THE CONTROL STRATEGIES BASED ON FUZZY LOGIC

Recently, a lot of researches intend to apply intelligent control theory to the control strategy of EV such as adaptive control [10], neural network [15] and fuzzy control [13]. Since fuzzy control is simple, easy to realize, no need for modelling and has strong robustness, it is suitable for nonlinear control where parameters and/or model are unknown or variable. It can converse engineers experience to control rules directly. Hence, it is very suitable for EV control. In this paper, the FLC with SMC of EMR is developed to invert the accumulation element associated with the chassis for estimating the reference of the total force  $F_{tot-ref}$ . The input parameters of FLC are the error and the change of error between  $V_{veh-mes}$  and  $V_{veh-ref}$  the output is the total reference force which corresponds to a torque reference to be applied to the motor as shown in Fig. 3

### 5.1 Fuzzy Logic System Design

FLS needs to define both input and output membership functions (MFs), fuzzification method, scaling factor values, type of membership, rules, rule processing (Mamdani, Sugeno), inference mechanism, and defuzzification method (Fig. 1) [14-16].

#### 5.1.1 Fuzzification Interface:

It will transform the input parameters, SOC, the signal U, the error  $\zeta$  and the change of error  $d\zeta/dt$  between  $v_{veh-ref}$  and  $v_{veh-mes}$  of the FLC from distinct quantity to fuzzy quantity. The nine-term sets are negative big (NB), negative average (NA), negative small (NS), zero negative (ZEN), zero (ZE), zero positive (ZEP), positive small (PS), positive average (PA) and positive big (PB) are used to define FLC output and inputs linguistic variables.

#### 5.1.2 Rule Base System:

The fuzzy rule base is a set of linguistic rules defined with IF-THEN conditions. The rule base which has the M number of rules ( $j=1, 2, \dots, M$ ) is shown in (14)[15].

$$R^j = \text{If } x_1 \text{ is } A_1^j \text{ and } x_2 \text{ is } A_2^j \text{ and } \dots \text{ and } x_n \text{ is } A_n^j \quad (14)$$

Then  $z$  is  $B^j$

$x_i$  ( $i=1, 2, \dots, n$ ) are the fuzzy system input parameters. The fuzzy output variables are denoted  $z$ . The membership functions  $\mu_{\zeta}(x_i)$  and  $\mu_{d\zeta/dt}(x_i)$  are represented as the input linguistic term  $A_i^j$ .  $B^j$  is the linguistic term for the fuzzy output [17,20]. All rule base system of FLC are shown on

TABLE 1. (15) shows the first rule assigned for the rule base system of FLC shown in TABLE I.

$$R^1 = \text{If } x_1 \text{ is } \mu_{\zeta}(N) \text{ and } x_2 \text{ is } \mu_{\frac{d\zeta}{dt}}(N) \quad (15)$$

Then  $F_{tot-ref}$  is NB

#### 5.1.3 Inference Machine:

According to the fuzzy quantity of input parameters, inference machine will find corresponding rules in rule base predefined, and use centrobaric method and minimum inference machine to get the output parameter [13] which is the fuzzy quantity of  $F_{tot-ref}$ . The simplest membership functions are adopted using straight lines. They are a Triangular and Trapezoidal membership for both input and output fuzzy sets. These straight line membership functions have the advantage of simplicity.

#### 5.1.4 Defuzzification Interface:

In defuzzification interface, the fuzzy output value in the fuzzy inference machine is converted into a non fuzzy output value. The actual value of FLC and FLS ( $F_{tot-ref}$ , range of FLC-MFs) are obtained by centroid defuzzification method [13].

## 6 SIMULATION RESULTS

The EV EMR is based on the one given by the L2EP lectures [11]. The MCS using and the FLC are directly converted into a Matlab/Simulink model as illustrated in Fig. 3. Indeed, by choosing appropriated inputs and outputs for subsystems, the action-reaction organization yields the block description of this software. The FLC was modelled using the matlab Fuzzy Toolbox with corresponding rules in rule base predefined. Triangular and Trapezoidal MFs were considered for both input and output fuzzy sets. Mamdani inference method was chosen for aggregation of activated rules with MIN function considered for AND operator. From the concept of EMR approach and its SMC, a reference velocity is imposed for the vehicle speed.

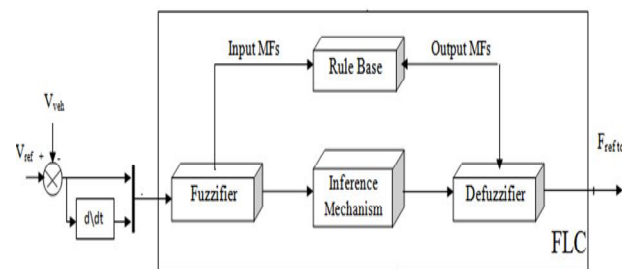


Figure 1: A typical structure of the Adaptive fuzzy logic control

**TABLE 1: The rules base system of FLC**

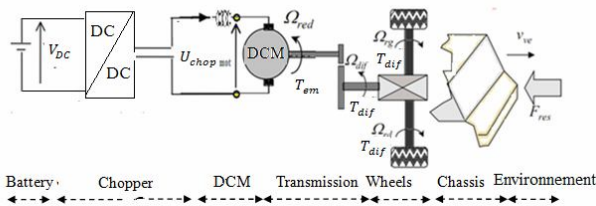
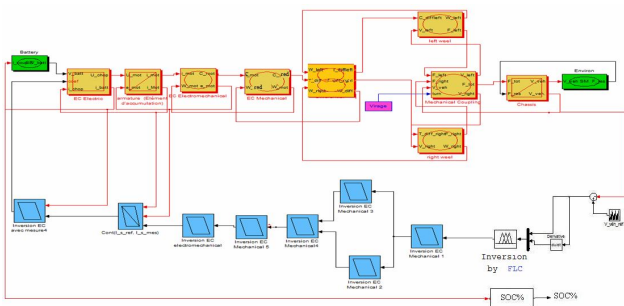
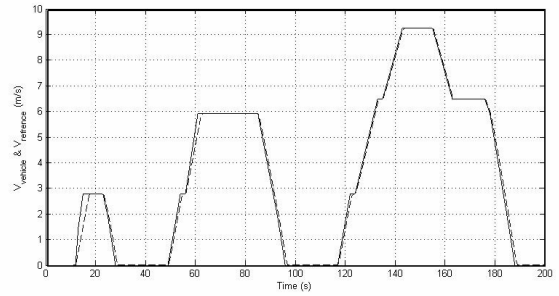
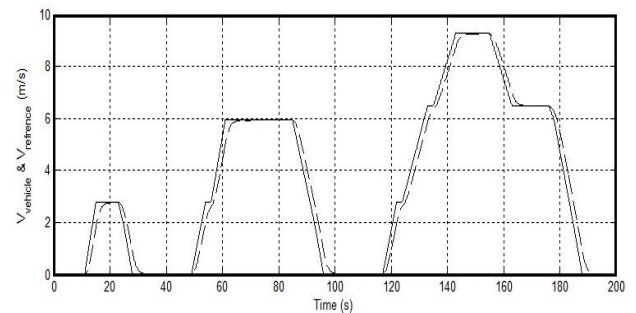
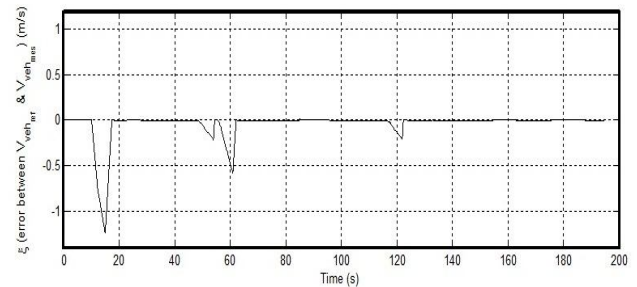
$\zeta$ $d\zeta/dt$	NB	NS	NA	ZE	PS	PA	PB
NB	NB	NB	NB	NA	NS	P	PB
NA	NB	NB	NA	NS	ZEN	ZEN	PS
NS	NA	NA	NS	ZE	ZEN	PS	PS
ZE	NS	ZEN	ZEN	ZE	ZE	ZEP	PS
PS	NS	NE	ZE	ZE	PS	PA	PB
PA	NS	ZE	PS	PS	PA	PB	PB
PB	PB	PS	PS	PA	PB	PB	PB

**TABLE 2: Parameters of DCM**

Parameter	Value
$P_{utilnom}$	32 kW
$L_{arm}$	0.0065H
$R_{arm}$	0.35W
$J_m$ (Rotor inertia)	0.12kg.m <sup>2</sup>

**ABLE 3: Parameters of EV body**

Parameter	Value
$M_{veh}$ (vehicle mass)	1000kg
$l_{veh}$ (rear wheel track)	1.6m
$d_{axe}$ (wheelbase)	2.4m
$R_{wheel}$ (Wheel radius)	0.52m
$J_{wheel}$ (Inertia of wheel)	4.3Kg.m <sup>2</sup>
$A_f$ (frontal surface of vehicle)	21.6m <sup>2</sup>
$\rho$ (Density of the air)	1.2Kg


**Figure 2: Components of studied architecture**

**Figure 3: EMR and SMC using FLC for the studied system under Matlab/Simulink [Adapted version of the given in 10]**

**Figure 4: Reference and vehicle velocities MCS with FLC**

**Figure 5: Reference and vehicle velocities MCS with IP**

**Figure 6: Error between the reference and vehicle velocities MSC with FLC**

At 65 s, the vehicle makes a turn during 3.46 s. The parameters of the DCM are given in Table 2. The main geometrical data and inertial properties of the vehicle and wheels are shown in Table 3.

The Fig. 4 shows a comparison between the reference and the vehicle velocity controlled using FLC on MCS of EMR. It can be seen that the vehicle velocity follows its reference, the steady state error is null as shown in Fig. 6. The same behavior for vehicle speed and its reference is obtained by using IP controller as shown in Fig. 5. Using the simulator EMR and SMC, the difference between the velocities of wheels is illustrated in Fig. 8. Indeed, when the vehicle makes a turn, the wheels left and right are not running at the same speed. When the left wheels slow down, the right wheels speed up to make the turn. Fig 8 shows the velocities of left and right wheels obtained using FLC on MCS. A very good control performance is obtained. The FLC membership functions were set off-line manually

regarding to two different vehicle operation modes. The first mode is a dynamic vehicle (sports vehicle) in which the response must be fast (Fig. 9), but does not safe consumption. The second corresponds an economic operations mode (Fig. 10), less dynamic is imposed in order to safe consumption and to obtain an economic (and not dynamic) vehicle. As shown in Fig. 9 and 10, the proposed method gives better results for both operation modes

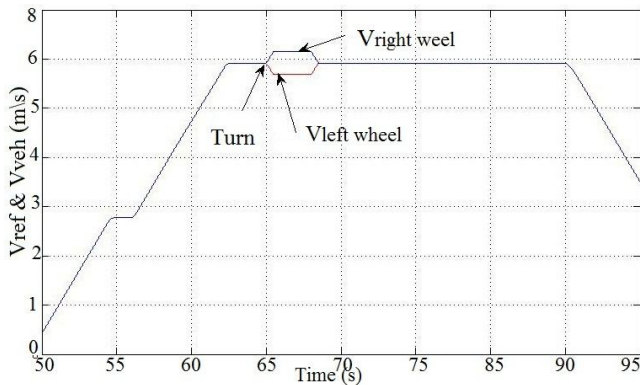


Figure 8: Left and right wheels vehicle velocities

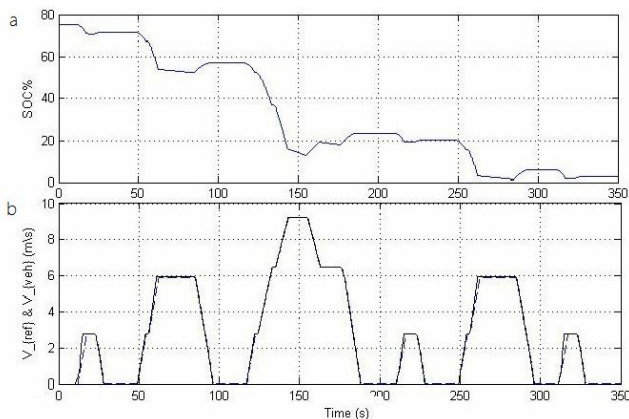


Figure 9 : (a) SOC% (b) Reference and vehicle velocities for the dynamic EV

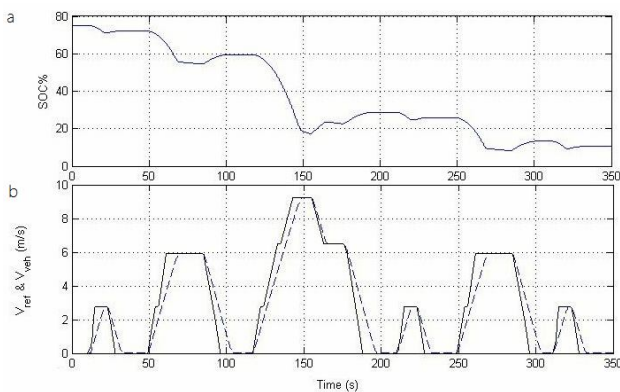


Figure 10: (a) SOC% (b) Reference and vehicle velocities for the economic EV

## 7 CONCLUSIONS

In this paper, the methodology of EMR, MCS and FLC for an EV were developed and presented for modelling and control of the EV purposes. The accumulation element inversion is generally done using the classic controllers (PI, IP or PID). These last need to adjust the value of their gains. This IP (or PI) gains determination is not easy and needs to be adjusted if the operating conditions change. This drawback of the MCS can be overcome using the presented FLC to invert these kinds of EMR elements. The FLC can be viewed as a nonlinear IP (or PID) controller where the parameters are automatically tuned according to the operating point. The proposed intelligent controller based on fuzzy logic system use minimum number of rules. This study shows a good agreement between the two types of MCS. The FLC can be dedicated entirely to MCS of dynamic system and it offers a robust and a realizable controller acting as a nonlinear PID.

## REFERENCES

- [1] WA. O'Brien, and RB. Stickel, and GJ. May, "Advancing electric vehicle development with pure-lead-tin battery technology", *Journal of power sources*, Elsevier. 1997 pp. 151-155.
- [2] G. S. Caux, W. Hankache, M. Fadel and D. Hissel, "On-line fuzzy energy management for hybrid fuel cell systems", *International Journal of Hydrogen Energy*, 1010, Elsevier. 1010. pp. 2134-2143.
- [3] L. Boulon, M.C. Pera, D. Hissel, A. Bouscayrol and P. Delarue "Energetic macroscopic representation of a fuel cell-supercapacitor system", *Vehicle Power and Propulsion Conference*, IEEE. 2007, pp. 290-297
- [4] A. Bouscayrol, X. Guillaud and P. Delarue, "Hardware-in-the-loop simulation of a wind energy conversion system using Energetic Macroscopic Representation", *Industrial Electronics Society*, IEEE. 2007. pp. 6-
- [5] A. Nouh, M. Chami, A. Djerdir and El M. Bagdouri, "Electric Vehicle Control using the Simulator ELEVES", *Vehicle Power and Propulsion Conference*, IEEE. 2007. pp. 696-701.
- [6] W. Lhomme, P. Delarue, P. Barrade and A. Bouscayrol, "Maximum control structure of a series hybrid electric vehicle using supercapacitors", *Proc. EVS21*, 2005. pp. 8.
- [7] O. Kraa, A. Aboubou, A. Henni, M. Becherif, M.Y. Mohammedi, M.Y. Ayad and M. Bahri, "Fuzzy Logic Based Maximum Control Structure of an Electric Vehicle", *International Conference on Renewable Energy : Generation and Applications*, IEEE-ICREGA12, United Arab Emirates 2012.
- [8] A. Bouscayrol, W. Lhomme, P. Delarue, B. Lemaire-Semail and S. Aksas, "Hardware-in-the-loop simulation of electric vehicle traction systems using Energetic Macroscopic Representation". *Conference on Industrial Electronics, 32nd Annual, IECON, IEEE 2006*. pp.5319--5324

- [9] W. Lhomme, A. Bouscayrol and P. Barrade, "Simulation of a series hybrid electric vehicle based on energetic macroscopic representation" *International Symposium on Industrial Electronics*, IEEE 2004. pp. 1525-
- [10] O. Kraa, M. Becherif, A. Aboubou, M.Y. Ayad, I. Tegani and A. Haddi, "Modeling and Fuzzy logic Control of Electrical Vehicle with an Adaptive Operation Mode", 4th International Conference on Power Engineering, Energy and Electrical Drives, IEEE-POWERENG13, Istanbul, Turkey, 2013.
- [11] Summer school on "Modelling and Control of electromechanical system using Energetic Macroscopic Representation Formalism", Labo. L2EP Lille 2005. France, <http://l2ep.univ-lille1.fr/commande/emr-2009/fr-presentation.htm>
- [12] A. Bouscayrol, A. Bruyère, P. Delarue, F. Girau, B. Lemaire-Semail, Y. Le Menach, W. Lhomme and F. Locment, "Teaching drive control using Energetic Macroscopic Representation-initiation level" *Conference on Power Electronics and Applications, 2007 European*, IEEE. pp. 1-9
- [13] S. Ashraf, E. Muhammad, A. Al-Habaibeh and F. Rashid, "Self learning fuzzy controllers using iterative learning tuner", *International Journal of Digital Signal Processing*, Elsevier. 2010. pp. 289-300.
- [14] H. Jabr, D. Lu, and N. Kar, "Design and Implementation of Neuro-Fuzzy Vector Control for Wind-driven Doubly-Fed Induction Generator", *IEEE Transactions on Sustainable Energy*, IEEE. 2011. pp. 1-1.
- [15] T. Nomura and T. Miyoshi, "An adaptive fuzzy rule extraction using hybrid model of the fuzzy self-organizing map and the genetic algorithm with numerical chromosomes", *Journal of Intelligent and Fuzzy Systems-Applications in Engineering and Technology*, IOS Press. 1998. pp. 39-52.